Journal of Molecular Catalysis A: Chemical 323 (2010) 7–15

Contents lists available at ScienceDirect

Journal of Molecular Catalysis A: Chemical

journal homepage: www.elsevier.com/locate/molcata

Editors choice paper

Selective oxidation of alcohols with molecular oxygen over Ru/CaO–ZrO_2 catalyst

Takashi Yasu-eda, Susumu Kitamura, Na-oki Ikenaga, Takanori Miyake, Toshimitsu Suzuki*

Department of Chemical Engineering and High Technology Research Center, Kansai University, 3-3-35 Yamate Suita, Osaka 564-8680, Japan

ARTICLE INFO

Article history:
Received 16 January 2010
Received in revised form 10 March 2010
Accepted 12 March 2010
Available online 21 March 2010

Keywords:
CaO–ZrO_2 solid solution
Ruthenium
Heterogeneous catalyst
Basic support
Oxidative dehydrogenation

ABSTRACT

Selective oxidation of alcohols to carbonyl compounds with molecular oxygen was carried out over ruthenium supported on a CaO–ZrO_2 solid solution prepared by the co-precipitation method. In the oxidation of benzyl alcohol, the Ru/CaO–ZrO_2 catalyst gave benzaldehyde in a yield higher than 98% at 90 °C, and the turnover frequency reached 224 h^{-1}. The Ru/CaO–ZrO_2 catalyst also exhibited high catalytic activities and selectivities to carbonyl compounds in the oxidation of aromatic ring-substituted benzylic, allylic, and aliphatic alcohols. Moreover, this catalyst exhibited high activities in the oxidation of alcohols at a low temperature (40 °C). The catalytic activity and oxidation state of ruthenium depended on the Ca/Zr molar ratio of the support, and the highest catalytic activity was obtained with Ca/Zr = 0.125. DRIFT and XPS analyses revealed that Ru^{n+}–OH (n = 3, 4) on the surface of CaO–ZrO_2 were likely the active species in the oxidation of alcohols.

1. Introduction

The selective catalytic oxidation of alcohols to the corresponding carbonyl compounds is one of the simplest and most important reactions in organic synthesis [1]. The oxidation has long been performed using a stoichiometric amount of various oxidants. From a *green chemistry* perspective, selective oxidation of alcohols using molecular oxygen has attracted much attention (Eq. (1)) [2–4]:

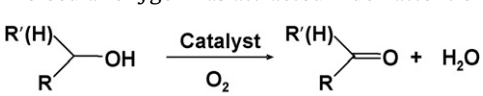

(1)

A wide range of homogeneous metal catalysts has been found to be useful for the oxidation of alcohols with molecular oxygen [5–8]. The use of heterogeneous catalysts, however, offers obvious advantages over homogeneous systems with respect to ease of handling and catalyst recycling. A wide range of supported platinum and palladium catalysts has long been reported to exhibit high catalytic performance in the oxidation of alcohols [2,9–11]. Pertinent review articles summarized recent development in this field [12,13].

Much attention has been paid to the application of supported ruthenium catalysts in alcohol oxidation. Various ruthenium-based catalysts such as Ru-exchanged hydroxyapatite (RuHAP) [14], Ru/Al_2O_3 [15–17], RuO_2/FAUzeolite [18], Ru-Co/Al_2O_3 [19], $RuMn_2$/hydrotalcite [20], RuCoHAP [21,22], RuHAP-γ-Fe_2O_3 [23], and Ru/TiO_2 [24,25] have been reported to be active and selective for benzylic, allylic, and aliphatic alcohols.

In general, Ru-hydroxide species (or hydrated RuOx species) are active in the oxidation of alcohols, although RuO_2 exhibits no catalytic activity [15–23]. Yamaguchi et al. reported that coordination number of nearest-neighbor Ru atoms closely related to the activity of Ru-loaded TiO_2 catalyst [24,25]. It has been reported that a reaction of $RuCl_3$ with basic sites on the support could generate Ru-hydroxide species, which in turn act efficient active sites for the oxidation of alcohols [20,26,27]. In addition, it is known that the basicity of the support plays an important role in the reaction [28–31]. As such, supports with a tunable basicity such as hydrotalcite or hydrotalcite-like mixed metal oxides seem to be preferable for the oxidation of alcohols [20,28–32].

Zirconium dioxide has been used in many catalytic reactions as a support material [33]. It is well known that the ZrO_2 can be stabilized by admixing with lower valence cations such as Y^{3+}, La^{3+}, Mg^{2+}, and Ca^{2+}. Replacement of the Zr^{4+} cation site with these cations leads to the formation of solid solutions and increases the number of oxygen vacancies [34]. Stabilized ZrO_2 has been reported to contain surface hydroxy groups that may behave as basic sites [35]. In particular, incorporation of Ca^{2+} into ZrO_2 leads to the formation of a homogeneous solid solution (CaO–ZrO_2) with a strong basic site. The basicity of the CaO–ZrO_2 solid solution can be controlled by changing its Ca/Zr molar ratio [36]. Various reactions using CaO–ZrO_2 solid solution-based catalyst such as autothermal reforming of CH_4 [37], synthesis of dimethyl carbonate and diethyl carbonate [38,39], CO_2 reforming of CH_4 [40], and steam reforming of ethanol [41] have been reported. In organic syntheses, however, no CaO–ZrO_2 solid solution-based catalysts have been reported.

In this report, we focus on the application of CaO–ZrO_2 solid solution as a support for the selective oxidation of alcohols to carbonyl compounds with molecular oxygen. We have found that

* Corresponding author. Tel.: +81 6 6368 1121x6807; fax: +80 6 6388 8869.
E-mail address: tmsuzuki5@yahoo.co.jp (T. Suzuki).

1381-1169/$ – see front matter © 2010 Elsevier B.V. All rights reserved.
doi:10.1016/j.molcata.2010.03.018

ruthenium supported on $CaO–ZrO_2$ affords a high catalytic activity with a high selectivity to carbonyl compounds. To the best of our knowledge, this work is the first report of liquid-phase oxidation using $CaO–ZrO_2$ solid solution-based catalysts.

2. Experimental

2.1. Catalyst preparation

$CaO–ZrO_2$ solid solution was prepared by co-precipitation method. $ZrO(NO_3)_2·2H_2O$ (4.5 g; Wako Pure Chemical Industries Ltd.) and a desired amount of $Ca(NO_3)_2·4H_2O$ (Wako Pure Chemical Industries Ltd.) were dissolved into 100 mL of water. The pH of the resulting solution was slowly adjusted to 13 by an addition of an aqueous solution of 1 mol/L NaOH under vigorous stirring. After 1 h, the resultant mixture was separated by centrifugation and the residue was washed with a large amount of water till neutral (pH < 8), and it was dried at 110 °C overnight. The solid mass was crushed and calcined at 600 °C for 5 h in air. Although the order of the addition of NaOH solution to the solution of Ca and Zr salts was reversed to the description in the literature [42], XRD patterns of the calcined oxides were exactly the same as those reported in the literature [42].

$RuCl_3·nH_2O$ (Ru 38.45 wt%, Mitsuwa Chemicals Co. Ltd.) was used as a ruthenium source. Ruthenium was introduced to the support (1.0 g) with 30 mL of an aqueous $RuCl_3$ solution (5.1×10^{-3} M) for 4 h at room temperature under stirring. After 4 h, the solid powder was again separated by centrifugation and washed with a large amount of water until no trace of Cl^- could be detected by $AgNO_3$ test. The powder remained was dried at room temperature under vacuum overnight and typically used without further pretreatment. The amount of ruthenium in the remaining solution was analyzed using inductively coupled plasma (ICP, Shimadzu ICPS-7510) to calculate the loading level of ruthenium on the catalyst. Ruthenium-supported hydrotalcite ($Mg_6Al_2(OH)_{16}CO_3·4H_2O$, Wako Pure Chemical Industries Ltd.) catalyst was prepared by the same procedure.

2.2. Oxidation of alcohols with molecular oxygen

The oxidation of alcohol was carried out in a 100 mL three-neck flask fitted with a reflux condenser. A catalyst (60–120 mg) was placed in the reactor and the reactor was purged with oxygen. Then 1–2 mmol of substrate, 5 mL of solvent (*o*-xylene) and 1–2 mmol of anisol (an internal standard: only in the cases to obtain time conversion profiles otherwise after the reaction) were introduced into the reactor through a septum. The reactor was immersed into a preheated oil bath, and stirring was started. The reaction was carried out by feeding pure oxygen directly into the liquid phase (10 mL/min).

After the reaction, the catalyst was separated by centrifugation. The products were analyzed by an FID-GC (Shimadzu model GC-18A) equipped with a 0.53 mm × 30 m capillary column of DB-WAXETR and were identified by a GC–MS (Shimadzu model QP2010) equipped with a 0.22 mm × 25 m capillary column of BP-21.

2.3. Catalyst characterization

Surface area of the supports and the catalysts were measured by the BET method using N_2 at −196 °C with an automatic Micromeritics Gemini 2375.

X-ray diffraction (XRD) measurements were performed with a Rigaku RINT-TTR III with monochromatized Cu Kα radiation.

Raman spectra were obtained with a Jasco model NSR-3000 laser Raman spectrometer using 523-nm diode laser excitation with a CCD detector.

The temperature-programmed desorption of CO_2 (CO_2-TPD) was performed with an automatic temperature-programmed desorption apparatus equipped with a quadrupole mass spectrometer as a detector (TPD-1-AT, Bel Japan Inc.). The sample was first treated at 700 °C for 30 min in flowing He. After cooling down to 100 °C in He, CO_2 was adsorbed onto the sample and was evacuated to remove excess CO_2. After cooling down to 50 °C in He, desorption of CO_2 was monitored at a heating rate of 5 °C/min to 850 °C in flowing He.

Diffuse reflectance infrared spectra (DRIFT) were recorded on a Jeol JIR 7000 in a diffuse reflectance mode. A KBr standard powder was used as the reference. Sixty-four scans were accumulated for each spectrum at a resolution of 4 cm^{-1}, and observed spectra were converted into Kubelka-Munk function units.

X-ray photoelectron spectroscopy (XPS) data were obtained on a Jeol JPS-9000MX using Mg Kα radiation. Powder samples were pressed and attached on carbon tape and mounted on a sample holder (Pt). The peaks were calibrated using the binding energy of Pt $4f_{7/2}$ (70.9 eV).

A Jeol JEM2010 was used to obtain high-resolution transmission electron microscope (HR-TEM) images at 200 kV.

3. Results and discussion

3.1. Characterization of $CaO–ZrO_2$ solid solution by XRD, Raman, and CO_2-TPD

Fig. 1 shows the results of XRD analyses of $CaO–ZrO_2$ mixed oxides with different Ca/Zr molar ratios (in charged Ca and Zr). Monoclinic (m-ZrO_2) and tetragonal (t-ZrO_2) structures exist on pure ZrO_2 (Fig. 1a). However, with the addition of Ca to ZrO_2

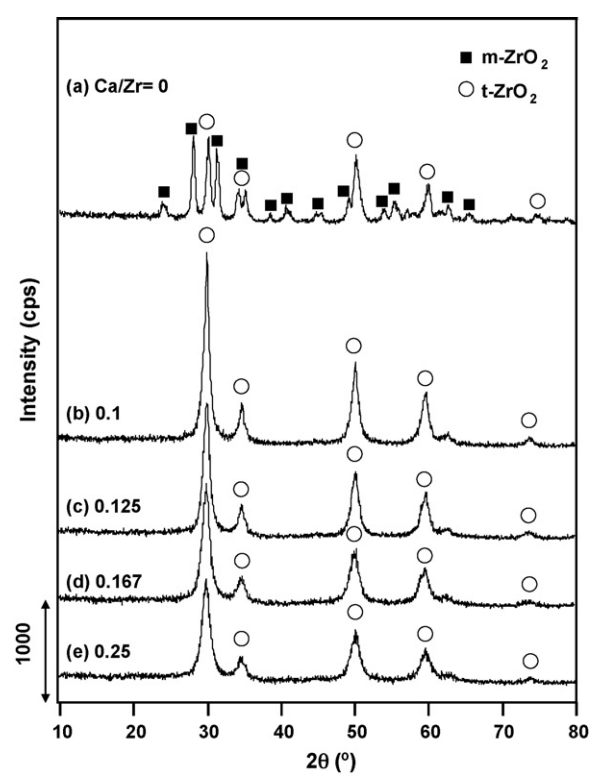

Fig. 1. XRD patterns of $CaO–ZrO_2$ solid solutions having various Ca/Zr molar ratios (numerals indicate molar ratio).

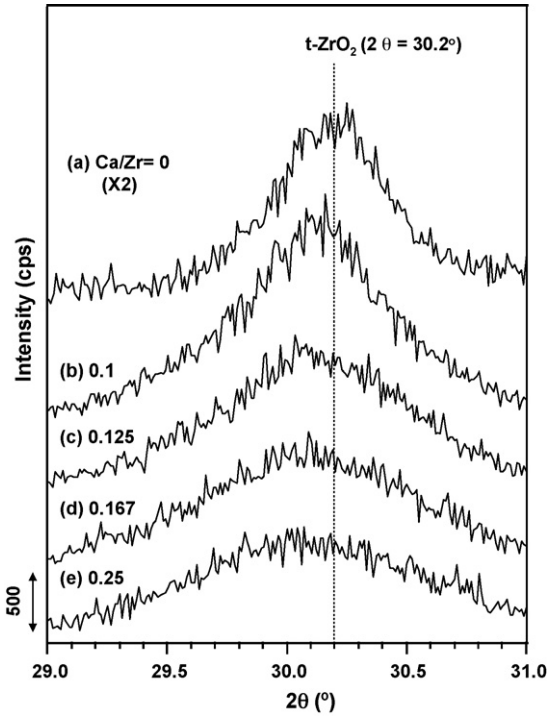

Fig. 2. High-resolution XRD patterns of CaO–ZrO_2 solid solutions having various Ca/Zr molar ratios (2θ = 29–31°).

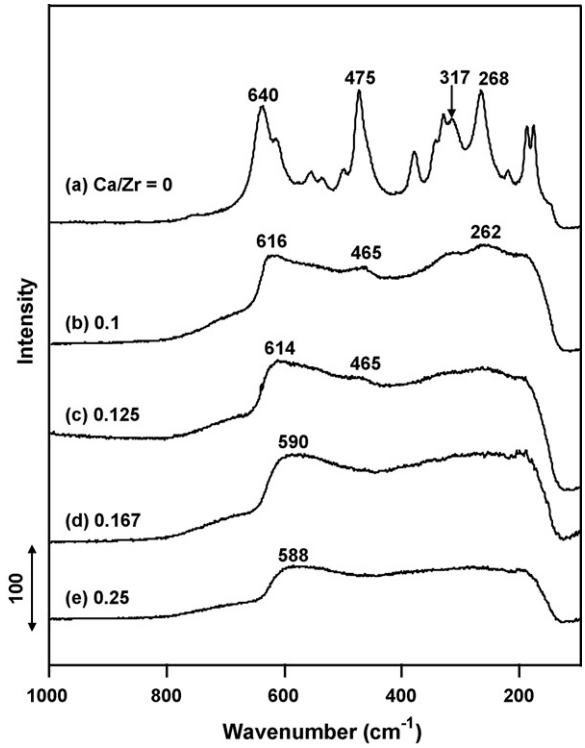

Fig. 3. Raman spectra of CaO–ZrO_2 solid solutions having various Ca/Zr molar ratios.

(Ca/Zr = 0.1–0.25 mol/mol), no monoclinic structure existed on the CaO–ZrO_2 mixed oxides, and only the tetragonal structure was observed (Fig. 1b–e). In these samples, CaO, $Ca(OH)_2$, and $CaCO_3$ could not be detected by XRD, though, with increasing Ca/Zr molar ratios, the diffraction peaks of t-ZrO_2 broadened. These results are in agreement with those observed in a CaO–ZrO_2 solid solution prepared by the glycothermal method [37]. It was reported that the formation of a homogeneous solid solution prevented a phase transformation from t-ZrO_2 to m-ZrO_2 and the growth of the crystallite size.

High-resolution XRD analyses of CaO–ZrO_2 between 2θ = 29–31° were carried out, and the results are shown in Fig. 2. The peak at 2θ = 30.2°, corresponding to the (1 1 1) reflection, shifted to a slightly lower angle with increases in the Ca/Zr molar ratio. Similar behavior has been observed in Y^{3+}-stabilized ZrO_2 [43], and also CaO–ZrO_2 solid solution [42]. The replacement of the Zr^{4+} cation with the Ca^{2+} cation slightly changes the lattice parameters of t-ZrO_2. Accordingly, we assumed that homogeneous CaO–ZrO_2 solid solution could be prepared by the precipitation method employed here.

Raman analyses of CaO–ZrO_2 solid solution with various Ca/Zr molar ratios are shown in Fig. 3. Raman peaks of m-ZrO_2 (at 178, 190, 222, 333, 382, 501, 539, 557 and 617 cm^{-1}) and t-ZrO_2 (at 268, 317, 475 and 640 cm^{-1}) were clearly observed on the pure ZrO_2 (Fig. 3a) [44]. In contrast, only very broad peaks corresponding to t-ZrO_2 were observed on the CaO–ZrO_2 solid solutions, and the peaks were further broadened with increases in the Ca/Zr molar ratio (Fig. 3b–e). The broadening of peaks might be ascribed to the larger number of oxygen vacancies existing in the CaO–ZrO_2 solid solutions.

In order to clarify the surface basicity of the CaO–ZrO_2 solid solutions, the CO_2–TPDs were performed and the results are shown in Fig. 4. The pure ZrO_2 had a small desorption peak at temperatures between 50 and 350 °C (Fig. 4a), which could be ascribed to the small number of weak basic sites on the ZrO_2 surface [36]. With increasing Ca/Zr molar ratios, the amounts of adsorbed CO_2 and the desorption temperatures clearly increased. The result indicates that the strong basic property of CaO affected the solid base characteristics of ZrO_2 [36].

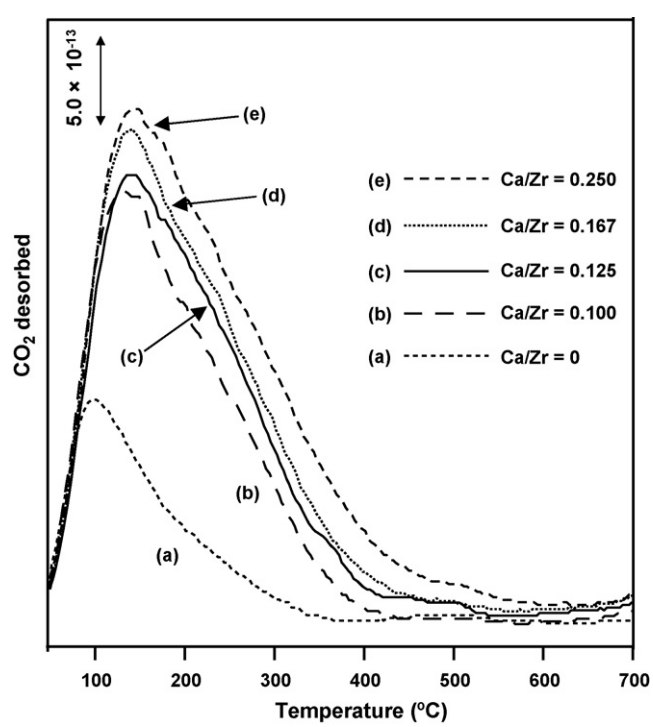

Fig. 4. CO_2-TPD profiles of CaO–ZrO_2 solid solutions having various Ca/Zr molar ratio. CO_2 adsorption: CO_2 100 Torr, 100 °C, 30 min; desorption: He 50 cm^3/min, 5 °C/min.

Table 1
Surface areas and Ru loading level of catalysts.

Catalyst	Ca/Zr[a] (mol/mol)	BET (m^2/g)		Ru (wt%)
		Support	Catalyst	
Ru/ZrO_2	0	42	–	<0.3
$Ru/CaO–ZrO_2$	0.100	125	132	0.8
$Ru/CaO–ZrO_2$	0.125	127	130	1.5
$Ru/CaO–ZrO_2$	0.167	138	138	1.5
$Ru/CaO–ZrO_2$	0.250	132	140	1.5

[a] Ca/Zr charged molar ratio.

3.2. Immobilization of Ru on $CaO–ZrO_2$ solid solution

Immobilization of ruthenium was performed by simply treating $CaO–ZrO_2$ solid solution with aqueous $RuCl_3$ solution at room temperature for 4 h. The amounts of immobilized ruthenium determined by ICP are shown in Table 1 together with the surface areas. As seen in Table 1, only a small amount of the ruthenium species was immobilized on the pure ZrO_2. However, with the addition of Ca^{2+} to the ZrO_2, ruthenium was immobilized onto the support. This result might be ascribed to the stronger basic property of the support with the addition of Ca^{2+}, leading to a reaction between ruthenium chloride and surface –OH group. As a result, the amount of ruthenium increased to 1.5 wt% (0.15 mmol/g) on the support at Ca/Zr = 0.125. Further increases in the Ca/Zr ratio increased numbers of basic site as discussed above, however, no significant increases in the Ru were observed. This may partly be ascribed to the increases in the basic site above Ca/Zr ratio 0.125 were small as compared to that without Ca to ratio 0.125. Therefore, increases in the amount of Ru immobilized to the catalyst surface seem to be within detection limit of analyses.

Changes in the BET surface areas were not observed in any of the samples before and after the immobilization of ruthenium.

3.3. Effect of Ca/Zr molar ratio and catalyst pretreatment on the oxidation of 1-phenylethanol

The effects of the Ca/Zr molar ratio and catalyst pretreatment on the oxidation of 1-phenylethanol over $Ru/CaO–ZrO_2$ catalyst were examined, and the results are shown in Table 2. Note that no by-product formation was observed and that the selectivity to acetophenone was higher than 98% with all the Ca/Zr molar ratios. The Ca/Zr molar ratio apparently influenced the catalytic performance of the $Ru/CaO–ZrO_2$, and the highest conversion of 1-phenylethanol (95%) was obtained with the molar ratio at Ca/Zr = 0.125 (entry 2). The relation between the catalytic activity and the Ca/Zr molar ratio may be ascribed to the changes in the basicity of the support [28–31].

Table 2
Effect of Ca/Zr molar ratio and catalyst pretreatment on the oxidation of 1-phenylethanol with molecular oxygen.[a].

Entry	Catalyst	Ca/Zr (mol/mol)	Ru (wt%)	Conv. (%)
1	$Ru/CaO–ZrO_2$	0.100	0.8	85
2	$Ru/CaO–ZrO_2$	0.125	1.5	95
3	$Ru/CaO–ZrO_2$	0.167	1.5	91
4	$Ru/CaO–ZrO_2$	0.250	1.5	77
5	$CaO–ZrO_2$[b]	0.125	–	No reaction
6	$Ru/CaO–ZrO_2$[c]	0.125	1.5	17
7	$Ru/CaO–ZrO_2$[d]	0.125	1.5	24

[a] 2 mmol 1-phenylethanol, $Ru/CaO–ZrO_2$ (11.9 μmol Ru), substrate/Ru = 168 mol/mol, 90 °C, 5 mL *o*-xylene, 2 h and O_2 flow (10 mL/min).
[b] 200 mg.
[c] Pretreated with air at 300 °C for 1 h.
[d] Pretreated with H_2 at 300 °C for 1 h.

It was found that the catalyst pretreatment with air or hydrogen at 300 °C greatly decreased the catalytic activity of $Ru/CaO–ZrO_2$ catalyst (entry 7 and 8). Opre et al. have reported that the pretreatment temperature of the catalyst is critical in the oxidation of benzyl alcohol with RuHAP and RuCoHAP catalysts due to the dehydration of active ruthenium species such as $Ru(OH)^{2+}$ [21]. The loss of catalytic activity in the $Ru/CaO–ZrO_2$ catalyst with pretreatment at an elevated temperature can be ascribed to the dehydration of active ruthenium species.

3.4. Characterization of catalysts by XRD, HR-TEM, DRIFT, and XPS

In the XRD analyses, no spectral differences between ruthenium-immobilized $CaO–ZrO_2$ catalysts and bare $CaO–ZrO_2$ solid solution were observed in any of the samples. The HR-TEM image of $Ru/CaO–ZrO_2$ catalyst was the same as that of bare $CaO–ZrO_2$ solid solution, and no particles of ruthenium species were identified. These results seem to indicate that ruthenium species are highly dispersed on the $CaO–ZrO_2$ solid solution.

In order to clarify the ruthenium species, DRIFT analyses were performed. A support having a Ca/Zr molar ratio of 0.125 was employed in this measurement. The left panel of Fig. 5 shows the DRIFT spectra of $CaO–ZrO_2$ solid solution (a), $Ru/CaO–ZrO_2$ as-prepared (b), $Ru/CaO–ZrO_2$ after treatment with D_2O at room temperature for 18 h (c), and $Ru/CaO–ZrO_2$ after treatment in air (d) and in H_2 at 300 °C (e). The difference spectra between $CaO–ZrO_2$ solid solution and respective samples are illustrated in the right panel of Fig. 5(f–i). The bare $CaO–ZrO_2$ solid solution showed a band at 3690 cm^{-1}, which can be assigned to the tri-bridging OH group of ZrO_2 [35,45]. Bands between 1300 and 1600 cm^{-1} are carbonate species originating from CO_2 adsorption from air [27,44]. Compared to the bare $CaO–ZrO_2$ solid solution (Fig. 5a), the intensities of a very broad band in the range 2500–3700 cm^{-1} and a band at 1630 cm^{-1} increased in the Ru-loaded catalysts (Fig. 5b and f). This behavior is similar to that reported for Ru/TiO_2 catalyst [46], and suggests the presence of adsorbed water on the catalyst.

After treatment with D_2O, the intensity of the band at 1630 cm^{-1} greatly decreased and the band $\nu_{O–H}$ in the range 2500–3700 cm^{-1} slightly weakened (Fig. 5c and g). Magnification of intensities in the region at 2200–2700 cm^{-1} revealed that adsorbed water on the catalyst surface was partly exchanged with D_2O and as a result the absorption shifted to 2500–2700 cm^{-1}. However, a large portion of the $\nu_{O–H}$ band in the range 2900–3700 cm^{-1} still remained after treatment with D_2O. This broad band in the range 2900–3700 cm^{-1} would be assigned to Ru–OH species [15–17] that could not be exchanged by the treatment with D_2O at an ambient temperature.

In contrast to the treatment with D_2O, the band in the range 2900–3700 cm^{-1} greatly decreased after the treatment in air and H_2 at 300 °C (Fig. 5d, e, h and i). These results indicate that the adsorbed water and Ru–OH were mostly removed by the treatment at an elevated temperature. These findings suggest that the active sites in the oxidation of alcohols are highly dispersed Ru–OH species on the $CaO–ZrO_2$ solid solution [15–23].

In addition, a new absorption was observed at 1840 cm^{-1} after treatment with air at 300 °C (Fig. 6c). This band seems to be the Ru^{4+}=O mode of the RuO_2 phase [27,46,47]. The result strongly supports that no RuO_2 species exists on the as-prepared catalyst.

Interestingly, the oxidation state of ruthenium species on $CaO–ZrO_2$ solid solution depended on the molar ratio of Ca/Zr. XPS profiles of the $Ru/CaO–ZrO_2$ catalysts with different Ca/Zr molar ratios are shown in Fig. 7. The Ru $3p_{3/2}$ peak of the $Ru/CaO–ZrO_2$ at the molar ratio of Ca/Zr = 0.1, appeared at a binding energy (BE) of 465.2 eV (Fig. 7a), which agrees with that reported for the RuHAP-γ-Fe_2O_3 catalyst involving monomeric Ru^{4+} species [23]. Oxidation of catalyst precursor Ru^{3+} to Ru^{4+} during the preparation of the

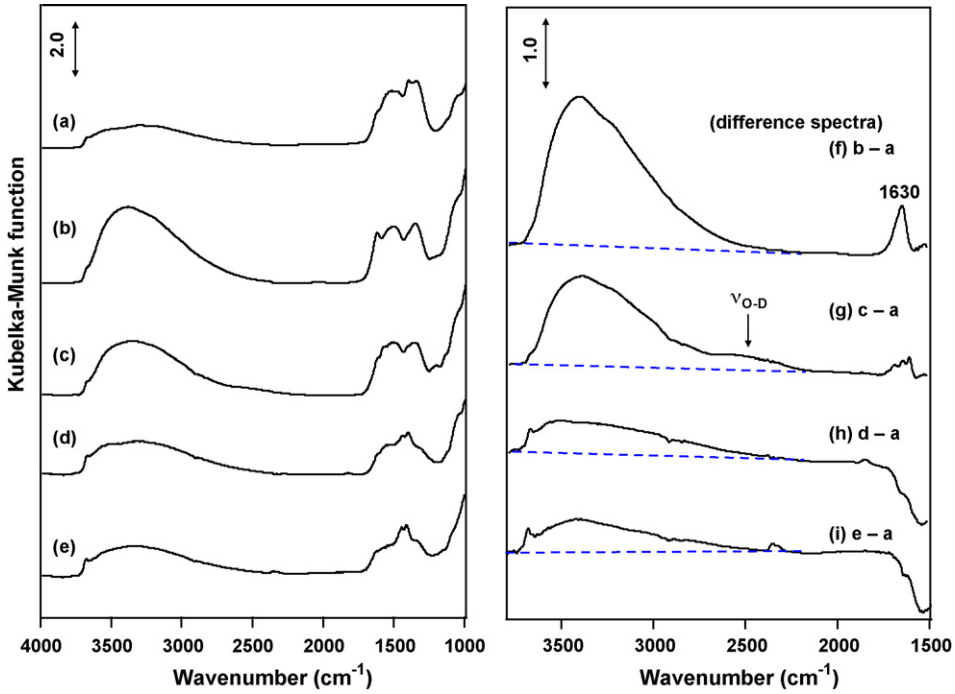

Fig. 5. Left panel: DRIFT spectra of a) $CaO–ZrO_2$ solid solution, b) as-prepared $Ru/CaO–ZrO_2$, c) $Ru/CaO–ZrO_2$ treated with D_2O, d) $Ru/CaO–ZrO_2$ treated in air at 300 °C for 1 h and e) $Ru/CaO–ZrO_2$ treated in H_2 at 300 °C for 1 h. Right panel: The difference spectra between $CaO–ZrO_2$ solid solution and respective spectrum shown in the left panel. A molar ratio of Ca/Zr = 0.125 was employed in all samples.

ruthenium-supported catalysts has been reported [18,20,23,26]. With an increase in the Ca/Zr molar ratio from 0.1 to 0.25, the Ru $3p_{3/2}$ peak shifted to a lower BE of 463.5 eV, assignable to Ru^{3+} species [14,17]. Two oxidation states of ruthenium species (Ru^{4+} and Ru^{3+}) seem to exist on the $Ru/CaO–ZrO_2$ at a molar ratio of 0.125 (Fig. 7b); this catalyst exhibited the highest catalytic activity in the oxidation of 1-phenylethanol.

A higher oxidation state of ruthenium (Ru^{4+}) has been reported to exhibit a high catalytic activity in the oxidation of alcohols [18–20,23]. In our study, however, no significant relation between the catalytic activity and the oxidation state of the ruthenium could

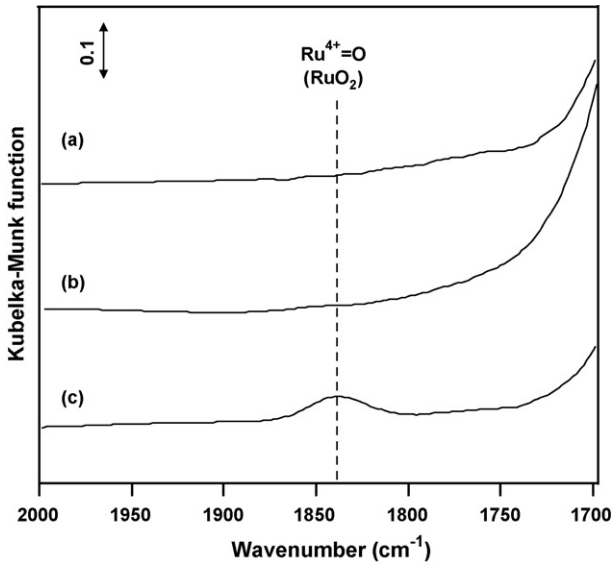

Fig. 6. DRIFT spectra of a) $CaO–ZrO_2$ solid solution, b) as-prepared $Ru/CaO–ZrO_2$, and c) $Ru/CaO–ZrO_2$ treatment in air at 300 °C for 1 h. The molar ratio Ca/Zr = 0.125 was employed in all samples.

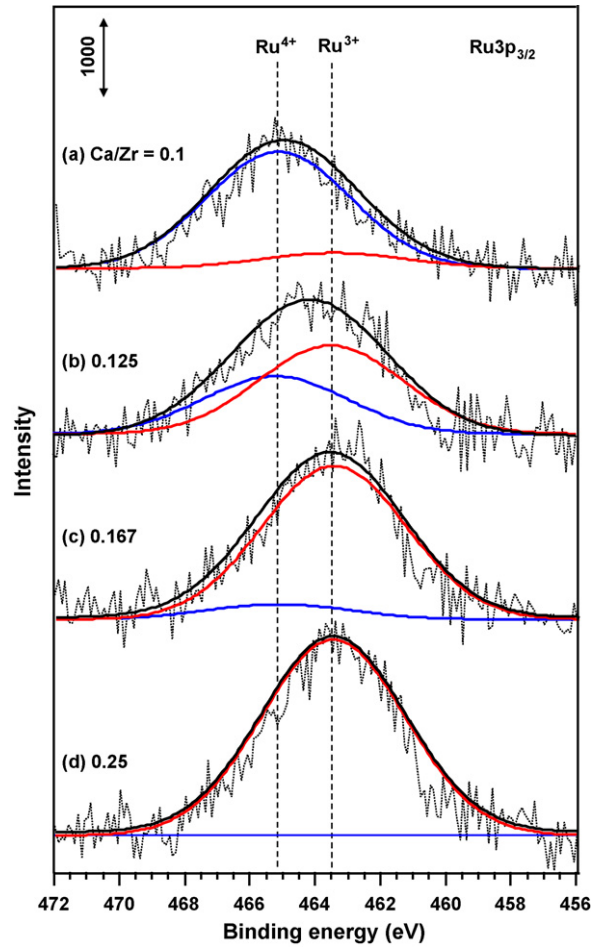

Fig. 7. XPS patterns of Ru $3p_{3/2}$ in $Ru/CaO–ZrO_2$ catalyst with various Ca/Zr molar ratios.

be observed, although the relative abundance of Ru^{3+} and Ru^{4+} shown in Fig. 7 obtained by curve fitting was not quantitative.

A probable explanation for the change in the BE (oxidation state of ruthenium) with the Ca/Zr molar ratio is the change in the interactions between ruthenium species and $CaO–ZrO_2$ solid solution. The dependency of the amount of immobilized ruthenium on the Ca/Zr molar ratio shown in Table 1 would support the change in such interactions. Slight increases in the amount of the more basic site on $CaO–ZrO_2$ at the ratio of 0.125 (compare the CO_2 desorption pattern at 350–500 °C) would likely be associated with the increase in the Ru loading level. Based on the XRD patterns of $Ru/CaO–ZrO_2$, the crystallite sizes of $CaO–ZrO_2$ decreased with an increase in the $CaO–ZrO_2$ ratio from 0.1 to 0.125, as seen in Fig. 1. Broadening of the diffraction peaks and the shift of the diffraction angle are more pronounced at Ca/Zr ratios from 0.1 to 0.125, indicating a co-relation between the $CaO–ZrO_2$ surface and the dispersion of loaded Ru species.

3.5. Oxidation of alcohols with molecular oxygen over $Ru/CaO–ZrO_2$ catalyst

Fig. 8 shows a conversion versus time profile for the oxidation of benzyl alcohol with molecular oxygen over $Ru/CaO–ZrO_2$ catalyst (Ca/Zr = 0.125 mol/mol) at 90 °C. The oxidation of benzyl alcohol was completed within 45 min, and benzaldehyde was obtained with ca. 100% yield without further oxidation to benzoic acid. The turnover frequency (TOF) based on the total amount of ruthenium

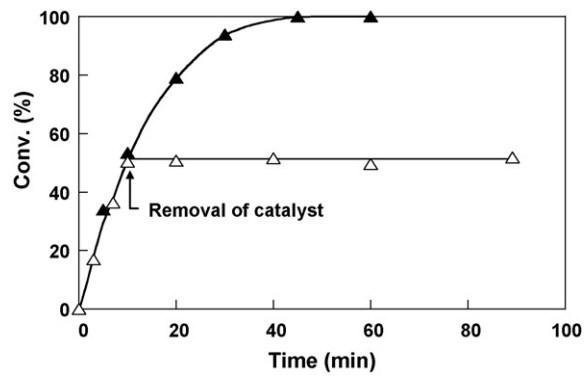

Fig. 8. Time vs. conversion profiles for the oxidation of benzyl alcohol with molecular oxygen over $Ru/CaO–ZrO_2$ catalyst and the effect of catalyst removal on conversion. Reaction conditions: 2 mmol benzyl alcohol, 80 mg $Ru/CaO–ZrO_2$ (Ca/Zr = 0.125 mol/mol, 11.9 μmol Ru), 90 °C, 5 mL *o*-xylene, O_2 flow (10 mL/min).

Table 3
Results of oxidation of various alcohols with molecular oxygen over $Ru/CaO–ZrO_2$ catalyst (Ca/Zr = 0.125).[a].

Entry	Substrate	Product	Substrate/Ru (mol/mol)	Time (h)	Conv. (%)	Yield (%)	TOF (h^{-1})
1	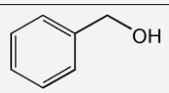	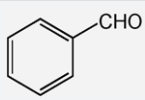	168	0.75	100	100	224
2[b]			168	0.75	Trace	Trace	–
3	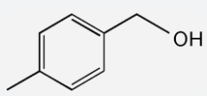	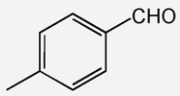	168	0.75	100	100	224
4	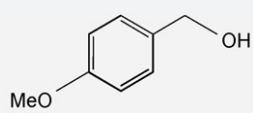	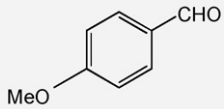	168	0.75	100	100	224
5	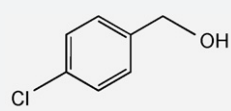	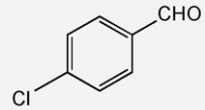	168	2.0	100	100	84
6	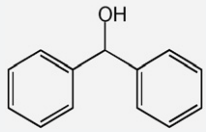	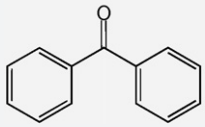	225	0.5	100	100	449
7	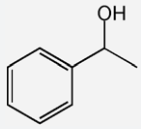	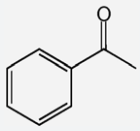	168	2.0	95	94	80
8	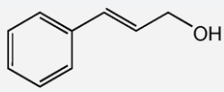	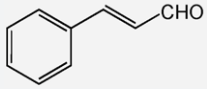	168	3.5	86	83	42
9[c]	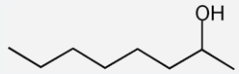	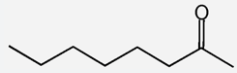	56	2.5	89	89	20

[a] 2 mmol substrate, 60–120 mg $Ru/CaO–ZrO_2$ (Ca/Zr = 0.125), 90 °C, 5 mL *o*-xylene and O_2 flow (10 mL/min).
[b] Under Ar atmosphere.
[c] 1 mmol substrate.

Table 4
The oxidation of benzyl alcohol,1-phenylethanol and cinnamyl alcohol with molecular oxygen over Ru/CaO–ZrO_2 catalyst (Ca/Zr = 0.125) at 40 °C.[a].

Entry	Substrate	Product	Time (h)	Conv. (%)	Yield (%)	TOF (h^{-1})
1	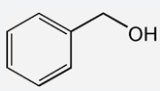	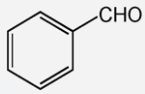	2	>99	>98	34
2	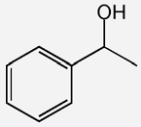	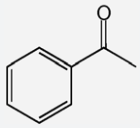	6	>99	>98	11
3	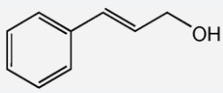	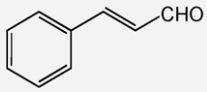	12	>99	>98	5.6

[a] 1 mmol substrate, 100 mg Ru catalyst (14.8 μmol Ru), substrate/Ru = 68 mol/mol, 40 °C, 5 mL *o*-xylene and O_2 flow (10 mL/min).

reached 224 h^{-1}. This value is slightly lower than that reported on Ru/HAP-modified with benzoic acid (TOF = 242 h^{-1} at 60 °C) [48] and higher than those reported for various ruthenium catalysts, including RuHAP (TOF = 2 h^{-1}, at 80 °C) [14], Ru/Al_2O_3 (40 h^{-1}, at 80 °C) [15], RuCoHAP (78 h^{-1}, at 90 °C) [21], RuCo/Al_2O_3 (80 h^{-1}, at 110 °C) [19], and RuHAP-γ-Fe_2O_3 (196 h^{-1}, at 90 °C) [23].

When the Ru/CaO–ZrO_2 catalyst was separated after the run for 10 min (conv. = ca. 50%), the oxidation of benzyl alcohol was completely terminated, as seen in Fig. 8 (Δ). This result strongly indicates that the oxidation of benzyl alcohol proceeded over the surface of the Ru/CaO–ZrO_2 catalyst, and that no leaching out of ruthenium species into the liquid phase occurred. Analysis of the supernatant solution by IPC after the reaction did not show even trace amount of Ru.

The Ru/CaO–ZrO_2 catalyst (Ca/Zr = 0.125 mol/mol) exhibited high performance in the oxidation of various alcohols (Table 3). Aromatic ring-substituted benzyl alcohols were converted into corresponding benzaldehydes in high yields (>98%) without further oxidation to substituted benzoic acids (entry 1 and 3–5). On the other hand, the oxidation of benzyl alcohol could not proceed under an Ar atmosphere (entry 2). The Ru/CaO–ZrO_2 catalyst also exhibited high catalytic activities in the oxidation of secondary benzylic alcohols (entry 6 and 7). It is noteworthy that the outstanding TOF value (449 h^{-1}) was obtained in the oxidation of diphenylmethanol (entry 6). The Ru/CaO–ZrO_2 catalyst also exhibited high activity in the oxidation of cinnamyl alcohol, which is commonly used as an example of allylic alcohol (entry 8). However, the selectivity to cinnamaldehyde slightly decreased (96%), since small amounts of by-products (3-phenyl-1-propanol and dihydrocinnamaldehyde) were formed by the hydrogenation of the C=C bond. This result suggests that Ru–H species were formed as an intermediate. A secondary aliphatic alcohol, 2-octanol, was also converted into 2-octanone with 89% yield, although the reaction rate was smaller than that of benzylic alcohols (entry 9).

We found that the Ru/CaO–ZrO_2 catalyst could be applied in the oxidation of alcohols even at 40 °C, as shown in Table 4. The benzylic and allylic alcohols were quantitatively converted into the corresponding carbonyl compounds with yields >98% with moderate reaction rates. In the oxidation of benzyl alcohol, the reaction was completed in 2 h and TOF up to 34 h^{-1} was obtained (entry 1). More recently, it was reported that Ru/MnOx/CeO_2 catalyst exhibits a high catalytic activity in the oxidation of alcohols at 30–60 °C [49]. Considering the TOF value in the oxidation of benzyl alcohol, our Ru/CaO–ZrO_2 catalyst system seems to be superior to the Ru/MnOx/CeO_2 catalyst (TOF = 22 h^{-1} at 40 °C). From these results, we believe that the Ru/CaO–ZrO_2 catalyst should be a preferred choice in the oxidation of alcohols to carbonyl compounds.

3.6. Reaction mechanism

The addition of 2,6-di-*tert*-butyl-*p*-cresol as a radical scavenger did not influence the rate and selectivity of the oxidation of benzyl alcohol. This result indicates that free-radical intermediates are not involved in the oxidation.

In order to better our understanding of the reaction mechanism, competitive oxidation of benzyl alcohol and 1-phenylethanol was performed (Scheme 1). The Ru/CaO–ZrO_2 catalyst gave benzaldehyde and acetophenone with 85 and 14% yield, respectively. Similar relative reactivity of the alcohols has been described in the literature with Ru/Al_2O_3 catalyst [15–17], and a larger oxidation rate of primary alcohols than secondary one seemed to indicate that sterically hindered Ru–alcoholate is involved as an intermediate [50,51]. Also, electron donating effect of alkyl group attached to –OH functional group may contribute smaller rate of H^- abstraction reaction.

The oxidation of several *p*-substituted benzyl alcohols was performed at 60 °C, and the Hammett plot at 60 °C is shown in Fig. 9. The slope of the Hammett plot ($\rho = -0.41$) was in agreement with those of RuHAP ($\rho = -0.43$) [14] and Ru/Al_2O_3 ($\rho = -0.46$) [16]. This result clearly indicates that β-hydride elimination is the rate-limiting step, as reported in the above references. In addition, the extremely high TOF for diphenyl methanol (entry 6 in Table 3), even the sterically hindered secondary alcohol, supports that β-hydrogen abstraction from Ru–alcohlate species is the rate determining step of this reaction, where inductive and resonance effects are involved. Recently Yamaguchi et al. provided clear evidence that β-hydride elimination is the rate-limiting step of Ru/TiO_2 catalyzed oxidation of alcohol, by using α-monodeuterobenzyl as substrate, where large kinetic isotope effects of k_H/k_D of ca. 5 were observed [25].

The effect of oxygen partial pressure on the oxidation of benzyl alcohol was examined at 90 °C (Fig. 10). Under 20%-O_2 in Ar, the reaction rate was smaller than that under a 100%-O_2 atmosphere.

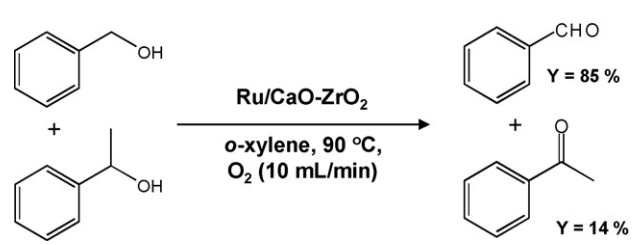

Scheme 1. Competitive oxidation of benzyl alcohol and 1-phenylethanol. Reaction conditions: 2 mmol benzyl acohol, 2 mmol 1-phenylethanol, 80 mg Ru/CaO–ZrO_2 (Ca/Zr = 0.125 mol/mol), 90 °C, 1 h, 5 mL *o*-xylene, O_2 flow (10 mL/min).

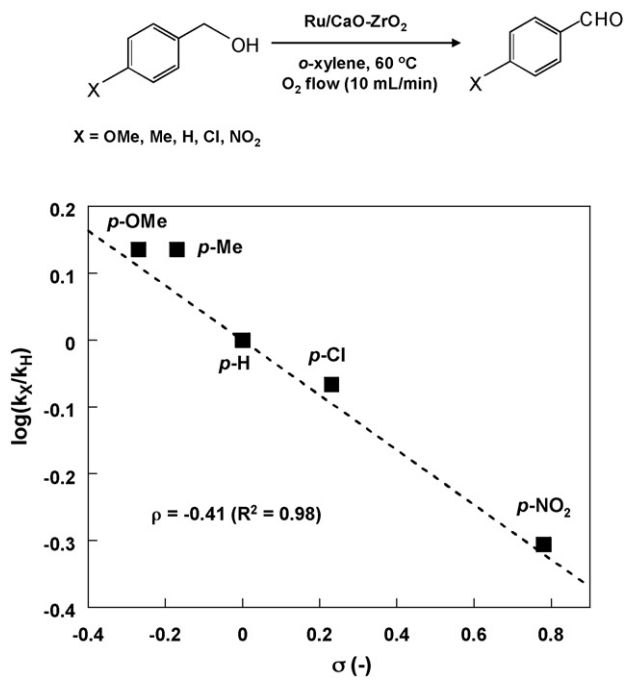

Fig. 9. Hammett plot of *p*-substituted benzyl alcohols. Reaction conditions: 1 mmol *p*-X-benzyl alcohol (X = OMe, Me, H, Cl, NO_2), 60 mg Ru/CaO–ZrO_2 (Ca/Zr = 0.125 mol/mol), 60 °C, 5 min, 5 mL *o*-xylene, O_2 flow (10 mL/min). σ values were taken from Ref. [52].

If pure O_2 was bubbled into the reaction mixture (10 mL/min), the reaction rate further increased. The dependence of the reaction rate on the oxygen partial pressure at a higher temperature suggests that the rate-limiting step changed from β-hydrogen abstraction to the re-oxidation of Ru–H species or oxygen mass transport [22].

Based on the results of our findings and literature data, we propose the reaction mechanism shown in Scheme 2 [15–20,22,23,25]. The first step is the formation of Ru–alcoholate species between Ru–OH species and alcohol together with the formation of H_2O (step 1). The Ru–alcoholate species undergoes β-hydride elimination to give a carbonyl compound and Ru–H species (step 2). The Ru–H species is then re-oxidized with molecular oxygen to give Ru–OOH species (step 3). Finally, the Ru–OOH species react with adsorbed H_2O on the support, followed by regeneration of the Ru–OH active phase via H_2O_2 formation (step 4). It was reported that H_2O_2 is unstable in the presence of a catalyst, and that decomposition of H_2O_2 is suppressed with H^+ [53]. Thus under the conditions employed here, even if H_2O_2 was formed, it decomposed

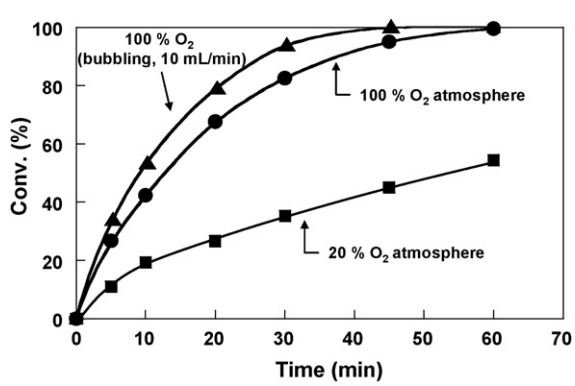

Fig. 10. Effect of oxygen partial pressure on the oxidation of benzyl alcohol. Reaction conditions: 2 mmol benzyl alcohol, 80 mg Ru/CaO–ZrO_2 (Ca/Zr = 0.125 mol/mol), 90 °C, 5 mL *o*-xylene.

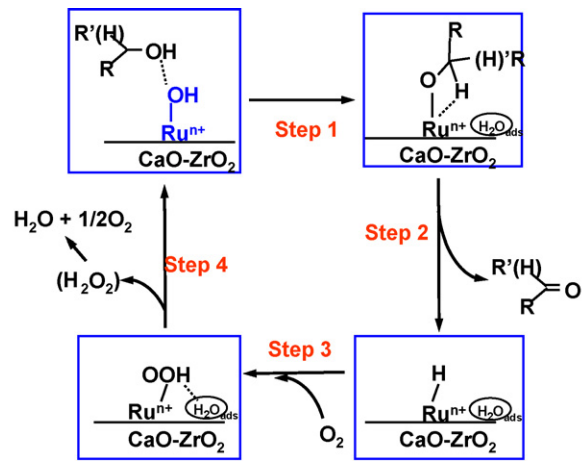

Scheme 2. Proposed reaction scheme for the oxidation of alcohols over Ru/CaO–ZrO_2 catalyst. Ru^{n+} should be $Ru^{3+} \sim Ru^{4+}$.

immediately and detection of it seems to be difficult. The same reaction scheme was proposed by Sheldon et al. [12]. Yamaguchi et al. proposed similar scheme without H_2O_2 formation [25].

Opre et al. have proposed a different pathway for this reaction. In their reaction path, a Ru^{n+}(H)–OH to $Ru^{n+}(OH)_2$ species has been proposed [22]. However, based on this route, a direct formation of molecular oxygen and Ru–H to Ru–OH from a Ru containing intermediate must be considered. Direct formation of molecular oxygen from the intermediate seems to be difficult, and our path involves more reasonable reaction courses. In the direct formation of H_2O_2 from oxygen and hydrogen, no Ru-based catalyst was proposed, indicating that free H_2O_2 could not be detected in the oxidation of alcohols.

4. Conclusion

Basic CaO–ZrO_2 solid solution was applied as a new support for Ru-loaded catalyst in the liquid-phase oxidation of alcohols. The highest activity was obtained with the support with a molar ratio of Ca/Zr = 0.125, and the Ru/CaO–ZrO_2 catalyst exhibited high catalytic performance in the oxidation of alcohols even at 40 °C. DRIFT and XPS analyses revealed that the Ru^{n+}–OH (n = 3, 4) seemed to be active species in the oxidation of alcohols.

We also found that the oxidation state of ruthenium species was affected by the Ca/Zr molar ratio. This relationship can be ascribed in part to the changes in the basicity of the solid solution, which change the interactions between loaded ruthenium and the support.

Acknowledgment

This work was financially supported in part by "High-Tech Research Center" Project for Private Universities: matching fund subsidy from MEXT, 2007-2011.

References

[1] R.A. Sheldon, J.K. Kochi, Metal-Catalyzed Oxidation of Organic Compounds, Academic Press, New York, 1981, p. 1.
[2] T. Mallat, A. Baiker, Catal. Today 19 (1994) 247.
[3] M. Besson, P. Gallezot, Catal. Today 57 (2000) 127.
[4] T. Mallat, A. Baiker, Chem. Rev. 104 (2004) 3037.
[5] K.P. Peterson, R.C. Larock, J. Org. Chem. 63 (1998) 3185.
[6] A. Dijksman, A. Mario-González, A.M. i Payeras, I.W.C.E. Arends, R.A. Sheldon, J. Am. Chem. Soc. 123 (2001) 6826.
[7] J. Muzart, Tetrahedron 59 (2003) 5789.
[8] S.S. Stahl, Angew. Chem. Int. Ed. 43 (2003) 3400.

[9] T. Mallat, Z. Bodnar, A. Baiker, O. Greis, H. Strubig, A. Reller, J. Catal. 142 (1993) 237.
[10] T. Mallat, Z. Bodnar, P. Hug, A. Baiker, J. Catal. 153 (1995) 131.
[11] K. Mori, T. Hara, T. Mizugaki, K. Ebitani, K. Kaneda, J. Am. Chem. Soc. 126 (2004) 10657.
[12] R.A. Sheldon, I.W.C.E. Arends, A. Dijksman, Catal. Today 57 (2000) 157.
[13] B.-Z. Zhan, A. Thomson, Tetrahedron 60 (2004) 2917.
[14] K. Yamaguchi, K. Mori, T. Mizugaki, K. Ebitani, K. Kaneda, J. Am. Chem. Soc. 122 (2000) 7144.
[15] K. Yamaguchi, N. Mizuno, Angew. Chem. Int. Ed. 41 (2002) 4538.
[16] K. Yamaguchi, N. Mizuno, Chem. Eur. J. 9 (2003) 4353.
[17] K. Yamaguchi, N. Mizuno, Catal. Today 132 (2008) 18.
[18] B.Z. Zhan, M.A. White, T.K. Sham, J.A. Pincock, R.J. Doucet, K.V.R. Rao, K.N. Robertson, T.S. Cameron, J. Am. Chem. Soc. 125 (2003) 2195.
[19] T.L. Stuchinskaya, M. Musawir, E.F. Kozhevnikova, I.V. Kozhevnikov, J. Catal. 231 (2005) 41.
[20] K. Ebitani, K. Motokura, T. Mizugaki, K. Kaneda, Angew. Chem. Int. Ed. 44 (2005) 3423.
[21] Z. Opre, J.-D. Grunwaldt, M. Maciejewski, D. Ferri, T. Mallat, A. Baiker, J. Catal. 230 (2005) 406.
[22] Z. Opre, J.-D. Grunwaldt, T. Mallat, A. Baiker, J. Mol. Catal. A: Chem. 242 (2005) 224.
[23] K. Mori, S. Kanai, T. Hara, T. Mizugaki, K. Ebitani, K. Jitsukawa, K. Kaneda, Chem. Mater. 19 (2007) 1249.
[24] K. Yamaguchi, T. Koike, J.W. Kim, Y. Ogasawara, N. Mizuno, Chem. Eur. J. 14 (2008) 11480.
[25] K. Yamaguchi, J.W. Kim, J. He, N. Mizuno, J. Catal. 268 (2009) 343.
[26] K. Motokura, D. Nishimura, K. Mori, T. Mizugaki, K. Ebitani, K. Kaneda, J. Am. Chem. Soc. 126 (2004) 5662.
[27] Z. Opre, D. Ferri, F. Krumeich, T. Mallat, A. Baiker, J. Catal. 251 (2007) 48.
[28] K. Kaneda, T. Yamashita, T. Matsushita, K. Ebitani, J. Org. Chem. 63 (1998) 1750.
[29] J.I. Di Cosimo, V.K. Diez, M. Xu, E. Iglesia, C.R. Apesteguia, J. Catal. 178 (1998) 499.
[30] P. Haider, A. Baiker, J. Catal. 248 (2007) 175.
[31] P. Haider, J.-D. Grunwaldt, R. Seidel, A. Baiker, J. Catal. 250 (2007) 313.
[32] T. Matsushita, K. Ebitani, K. Kaneda, Chem. Commun. (1999) 265.
[33] K. Tanabe, T. Yamaguchi, Catal. Today 20 (1994) 185.
[34] R.C. Garvie, J. Am. Ceram. Soc. 51 (1968) 553.
[35] J. Zhu, J.G. van Ommen, L. Lefferts, Catal. Today 117 (2006) 163.
[36] S. Liu, J. Ma, L. Guan, J. Li, W. Wei, Y. Sun, Micropor. Mesopor. Mater. 117 (2009) 466.
[37] T. Takeguchi, S.-N. Furukawa, M. Inoue, K. Eguchi, Appl. Catal. A.: Gen. 240 (2003) 223.
[38] H. Wang, M. Wang, N. Zhao, W. Wei, Y. Sun, Catal. Lett. 105 (2005) 253.
[39] H. Wang, M. Wang, W. Zhang, N. Zhao, W. Wei, Y. Sun, Catal. Today 115 (2006) 107.
[40] S. Liu, L. Guan, J. Li, N. Zhao, W. Wei, Y. Sun, Fuel 87 (2008) 2477.
[41] J.D.A. Bellido, E.M. Assaf, J. Power Sources 177 (2008) 24.
[42] H. Wang, M. Wang, S. Liu, N. Zhao, W. Wei, Y. Sun, J. Mol. Catal. A Chem. 258 (2006) 308.
[43] J.D.A. Bellido, E.M. Assaf, Appl. Catal. A.: Gen. 352 (2009) 179.
[44] C.L. Oieck, M.A. Banares, M.A. Vicente, J.L.G. Fierro, Chem. Mater. 13 (2001) 1174.
[45] B. Bachiller-Baeza, I. Rodriguez-Ramos, A. Guerrero-Ruiz, Langmuir 14 (1998) 3556.
[46] A. Köckritz, M. Sebek, A. Dittmar, J. Radnik, A. Brückner, U. Bentrup, M.-M. Pohl, H. Hugl, W. Mägerlein, J. Mol. Catal. A: Chem. 246 (2006) 85.
[47] K. Hadjiivanov, J.-C. Lavalley, J. Lamotte, F. Maugé, J. Saint-Just, M. Che, J. Catal. 176 (1998) 415.
[48] Z. Opre, D. Ferri, F. Krumeich, T. Mallat, A. Baiker, J. Catal. 241 (2006) 287.
[49] T. Sato, T. Komanoya, Catal. Commun. 10 (2009) 1095.
[50] S. Kanemoto, S. Matsubara, K. Takai, K. Oshima, K. Utimoto, H. Nozaki, Bull. Chem. Soc. Jpn. 61 (1988) 3607.
[51] G.J. ten Brink, I.W.C.E. Arends, R.A. Sheldon, Adv. Synth. Catal. 344 (2002) 355.
[52] C. Hansch, A. Leo, R.W. Taft, Chem. Rev. 91 (1991) 165.
[53] C. Samanta, Appl. Catal. A: Gen. 330 (2008) 133.